Applied Catalysis B: Environmental 90 (2009) 395–404

Contents lists available at ScienceDirect

Applied Catalysis B: Environmental

journal homepage: www.elsevier.com/locate/apcatb

A combined DRIFTS and MS study on reaction mechanism of NO reduction by CO over NiO/CeO_2 catalyst

Xiaoqing Cheng [a], Aimin Zhu [a], Yuzhuo Zhang [a], Yong Wang [a], C.T. Au [c], Chuan Shi [a,b,*]

[a] Laboratory of Plasma Physical Chemistry, Dalian University of Technology, Dalian 116024, PR China
[b] State Key Laboratory of the Fine Chemicals, Dalian University of Technology, Dalian 116024, PR China
[c] Department of Chemistry, Hong Kong Baptist University, Kowloon Tong, Hong Kong, China

ARTICLE INFO

Article history:
Received 15 January 2009
Received in revised form 6 March 2009
Accepted 24 March 2009
Available online 10 April 2009

Keywords:
NiO/CeO_2 catalyst
NO–CO
NCO complexes
DRIFTS
MS

ABSTRACT

Previously, we reported the prominent catalytic activity of ceria-supported nickel oxide catalyst for the reduction of NO by CO [Y. Wang, A.M. Zhu, Y.Z. Zhang, C.T. Au, X.F. Yang, C. Shi, Appl. Catal. B 81 (2008) 141–149]. In the present study, the reaction mechanism of NO and CO over the NiO/CeO_2 catalyst has been examined in two kinds of reaction modes: (i) NO reaction with CO pre-treated catalyst and (ii) CO reaction with NO pre-treated catalyst, by employing *in situ* diffuse reflectance infrared Fourier transform spectroscopy (DRIFTS) coupled with mass spectroscopy (MS) techniques. It was found that the generation of surface NCO complexes and N_2 (g) occurs only in mode (i), which gives obvious evidence of NO dissociation over CO pre-reduced NiO/CeO_2 catalyst. The result is similar to that obtained in the case of NO and CO co-adsorption, but different from that of mode (ii). The overall results indicate that CO reduction of surface oxygen should be the first and crucial step, and the dissociation of NO on the CO-reduced surface is a pathway for N_2 generation. The other pathway for N_2 generation is the interaction of NCO complexes with NO. Based on these understandings, we proposed reaction steps for the catalytic reduction of NO by CO over the NiO/CeO_2 catalyst.

1. Introduction

Carbon monoxide (CO) and nitric oxide (NO) are major air pollutants. The removal of them from automobile exhausts has been an important subject in environmental catalysis. In a conventional three-way catalytic converter, Pt, Rh and Pd are commonly used [1–5]. Due to the high costs of precious metals, considerable efforts have been paid to the utilization of cheaper transition metals and their oxides, and cases such as V [6,7], Cu [8–11], Ag [12,13], Cr [14–16], Co [17] have been reported.

In our previous paper, we reported that the CeO_2-supported NiO catalyst exhibits high activity for NO reduction by CO under stoichiometric conditions in the absence as well as in the presence of oxygen [18]. The interfacial synergism of nickel and ceria as evidenced by the generation of oxygen species that can be easily reduced has been proposed to be the reason for the high catalytic activities.

For a better understanding of mechanistic details, investigation of the formation and reactivity of surface intermediates is crucial. Combining FTIR spectroscopy and mass spectroscopy is an effective approach that permits simultaneous monitoring of gas-phase composition and the evolution of surface species on the catalyst. Almusaiteer et al. [19,20] studied the dynamic behavior of adsorbed NO and CO under transient NO–CO reaction conditions over Pd/Al_2O_3 by *in situ* IR spectroscopy coupled with TPR and pulse reaction techniques. The study demonstrated that careful selection of transient IR techniques allows (i) determination of the modes of adsorbed NO and CO participating in the reaction, and (ii) development of a comprehensive mechanism for NO–CO reaction. Chafik and co-workers [21–23] examined the formation, stability, and reactivity of surface isocyanate species with NO, CO, and O_2 over Rh/TiO_2 (W^{6+}) catalysts using FTIR and transient MS techniques. It has been found that W^{6+} doping of TiO_2 results in stabilization of the Rh-NCO species, and surface isocyanates react with NO to yield gaseous N_2O, providing an alternative route for N_2O production. Recently, FTIR combined with MS was used to follow the NO–CO reaction and the formation of NCO surface complexes over Rh/CeO_2 [24]. It was suggested that the NCO species formed on Rh spilled over onto CeO_2 where they remained stable.

* Corresponding author at: Laboratory of Plasma Physical Chemistry, Box 288, Dalian University of Technology, Dalian 116024, PR China.
Tel.: +86 411 84708548×803; fax: +86 411 84708548×808.
E-mail address: chuanshi@dlut.edu.cn (C. Shi).

0926-3373/$ – see front matter © 2009 Elsevier B.V. All rights reserved.
doi:10.1016/j.apcatb.2009.03.033

As to the mechanistic aspects of NO–CO reaction, it is generally believed that there are two kinds of modes: one involves NO dissociative adsorption [21,25–27] and the other is catalyst-assisted decomposition of molecularly adsorbed NO in the presence of a reductant [28,29]. On catalysts of copper oxides [30–34], which have been a focus of investigation among non-noble metal catalyst, the reduction of NO in the presence of CO is believed to proceed in two steps, first partial reduction of NO to give N_2O, and then subsequent reduction of N_2O to N_2. The results of the present investigation indicated the involvement of dissociative adsorption of NO. Accordingly, we proposed reaction pathways that involve the corresponding modes of NO and CO participation in NO reduction by CO.

2. Experimental

2.1. Materials

The CeO_2 sample was prepared by homogenous precipitation. The CeO_2-supported NiO catalysts were prepared via wetness impregnation using $Ni(NO_3)_3{\cdot}6H_2O$ as precursor (to give a final nickel loading of 7 wt%). The obtained samples were dried in an oven at 120 °C for over 8 h, pressed, sieved, and finally calcined at 500 °C for 1 h in He before being tested.

2.2. Techniques

All gases (NO/He, CO/He, and He) used were of ultra-high purity. Helium was purified using oxygen traps. DRIFTS analysis of adsorbed species on the catalyst surface under reaction conditions was carried out over a Bruker TENSOR 27 spectrometer equipped with a LATGS detector. The resolution of the spectrum (128-scan) was 4 cm^{-1}. A DRIFT cell fitted with CaF_2 beam splitter and heating cartridge was used to facilitate the control of temperature and gas atmosphere. The fine catalyst powder placed on a sample holder was carefully flattened to enhance IR reflection. With the sample securely located in the cell and under a flow of helium, the catalyst was calcined at 500 °C for 1 h and then cooled to 170 °C in flowing He. The cell was then directly connected to a flow system that allowed convenient switch of feed gases for transient studies. Gas feed of 1% CO/He or 1% NO/He composition (flow rate = 20 cm^3 min^{-1}) was adopted for the stepwise adsorption and subsequent NCO species reaction processes. For co-adsorption investigations, the composition of feed was 0.5% CO–0.5% NO/He (flow rate = 50 - cm^3 min^{-1}), and the gas used in the subsequent NCO species reaction process was 0.08% CO/He or 0.08% NO/He (flow rate = 50 cm^3 min^{-1}).

An online mass spectrometer (MS, Omini-star, GSD-300) equipped with a fast-response inlet capillary/leak diaphragm system along with an infrared absorption spectrometer (IRAS, SICK-MAIHAK, S710) was used to analyze effluent gases. Since CO and N_2 are of m/z = 28, while CO_2 and N_2O of m/z = 44, the two pairs of gaseous molecules cannot be analyzed by MS alone. Therefore, the presence of CO, N_2O and CO_2 in the gas phase was determined by IRAS. The composition of the feed used in the stepwise adsorption process was 0.08% CO/Ar or 0.08% NO/Ar. That of the feed adopted in the NCO species reaction process was 0.08% CO/He or 0.08% NO/He. In co-adsorption processes, the composition of feed used was 0.5% CO–0.5% NO/He and the flow rate was 50 cm^3 min^{-1}. The flow rate of carrier gas for MS measurement was 50 cm^3 min^{-1}. The MS signals at m/z = 28 (CO^+ and N_2^+), 30 (NO^+), 32 (O_2^+) and 44 (CO_2^+ and N_2O^+) were recorded continuously. When necessary (e.g. for the analysis of signal intensities of CO_2 and CO), the cracking coefficient determined in separate standard experiments was taken into account.

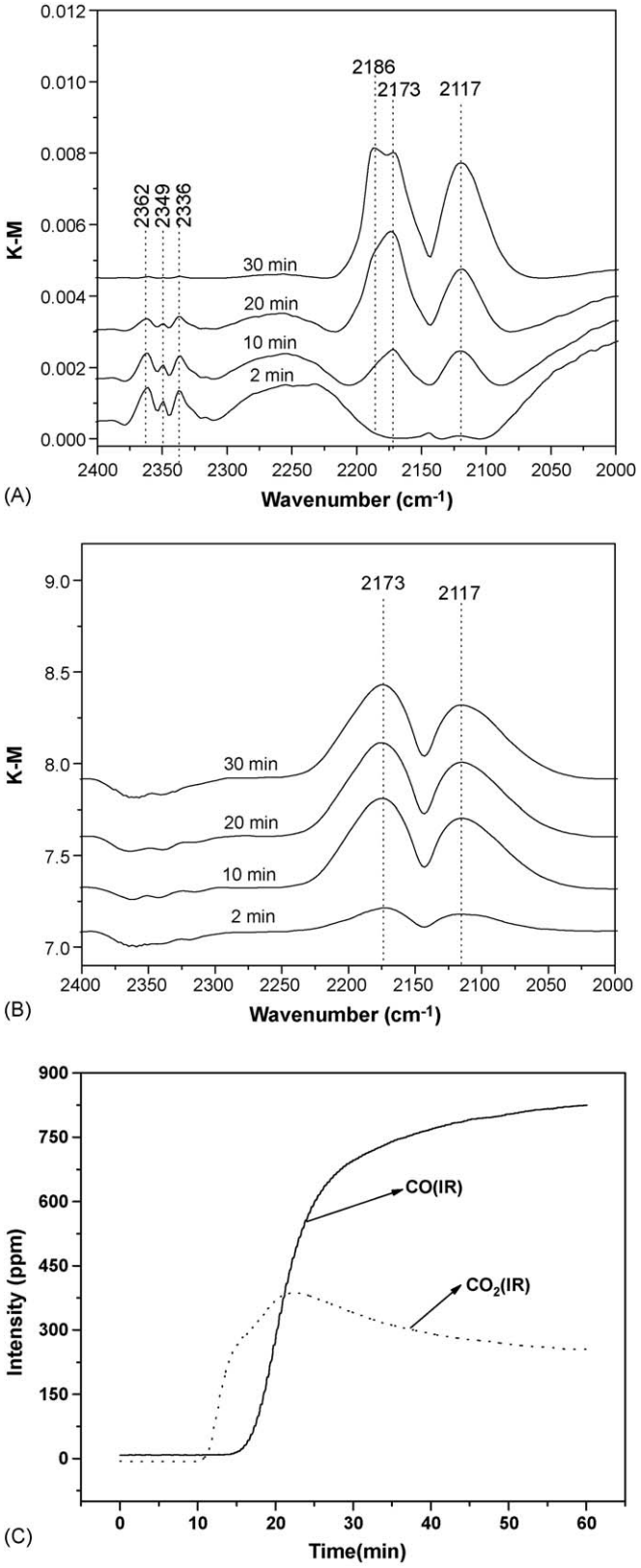

Fig. 1. DRIFT spectra (2400–2000 cm^{-1}) as a function of time when NiO/CeO_2 (A) and CeO_2 (B) was exposed to 1% CO/He; and IR responses of gas phase CO, CO_2 obtained when a NiO/CeO_2 sample was exposed to a flow of 0.08%CO/Ar at 170 °C (C).

3. Results

3.1. Combined DRIFTS and MS studies of stepwise exposure to NO and/or CO

3.1.1. CO adsorption on NiO/CeO_2 catalyst

The DRIFT spectra obtained upon exposure of the NiO/CeO_2 catalyst to 1% CO/He gas stream at 170 °C are shown in Fig. 1(A). At the beginning of exposure, bands assignable to adsorbed CO_2 are detected at 2362, 2349 and 2336 cm^{-1}. With time on steam, these bands decrease in intensity and new bands appear at 2186, 2173 and 2117 cm^{-1}. After 30 min of exposure, the spectrum is dominated by intense absorption bands located at 2186, 2173 and 2117 cm^{-1}. Exposing a CeO_2 sample to a flow of 1% CO/He at 170 °C would result in the detection of two intense bands, one at 2173 cm^{-1} and the other at 2117 cm^{-1} (Fig. 1(B)). According to Kladis et al. [35], these two bands are due to asymmetric and symmetric vibration of $Ce^{3+}(CO)_2$. With such understanding, we ascribe the 2173 and 2117 cm^{-1} bands of Fig. 1(A) to asymmetric and symmetric vibration of $Ce^{3+}(CO)_2$, respectively. The 2186 cm^{-1} band observed over NiO/CeO_2 is not detected over pure CeO_2. Before, Mihaylov et al. [36] attributed the band at 2185 cm^{-1} obtained after exposing NiO/ZrO_2 to CO to Ni^{2+}–CO complexes. We hence ascribe the 2186 cm^{-1} band to CO adsorbed on nickel species. A comparison between Fig. 1(A and B) reveals that there is surface CO_2 on NiO/CeO_2 but not on CeO_2. The results of online IRAS experiment (Fig. 1(C)) show the formation of CO_2 (g) when the NiO/CeO_2 catalyst was exposed to CO, in good agreement with the DRIFTS results. The CO_2 profile comes to a maximum after 20 min, and then declines gradually with time. At about 30 min, the CO signal intensity returns to that of the feed, indicating the end of CO interaction with the catalyst.

3.1.2. NO interaction with CO pre-treated catalyst

After purging with He for 5 min, the NiO/CeO_2 catalyst saturated with CO is exposed to 1% NO/He at 170 °C (Fig. 2(A and B)). The switch results in distinct changes in IR spectra. The strong overlapped bands at 2186 and 2173 cm^{-1} as well as the band at 2117 cm^{-1} disappear. As a result, the intense bands at 2210 and 2237 cm^{-1} become clearly visible. The 2210 and 2237 cm^{-1} bands come to a maximum after 5 min and then decreases in intensity with time. There are lots of reports on NCO formation over metal oxides (TiO_2, MgO, Al_2O_3 and SiO_2) [37–40], and it has been pointed out that asymmetric stretch of NCO sensitively depends on the nature of support. According to Bánsági et al. [24], HNCO adsorption on pure CeO_2 at 300 K yields bands at 2210 and 2180–2184 cm^{-1} attributable to isocyanate species that bond to CeO_2. They also reported the formation of NCO surface complexes over Rh/CeO_2, and the accumulation and stabilization of NCO on CeO_2 after NCO spillover from Rh. Thus, it is reasonable for us to ascribe the band at 2210 cm^{-1} to NCO complexes on CeO_2. The band at 2237 cm^{-1} is due to surface N_2O [35,41].

Apart from the bands mentioned above, switching of feed to NO also results in the appearance of a band at 1815 cm^{-1} that is not observed over pure CeO_2. We assign this band to Ni^{+}–NO complexes since Mihaylov et al. [36] attributed such a band to Ni^{+}–NO complexes before. The bands in the region of 1600–1450 cm^{-1} are due to C- and N-containing species associated with the support [[22] and the references therein].

The results of the corresponding MS-IRAS experiments are presented in Fig. 2(C). It is observed that during the first 1 min after exposure to NO, only N_2 appears at the exit of the reactor. At ca. 3 min, there is the detection of CO_2 in the effluent. Then NO begins to evolve at ca. 20 min, and the yields of N_2 and CO_2 start to decline. Accompanied by the appearance of NO is the formation of N_2O, and the N_2O yield comes to a maximum at 26 min and then drops. After 30 min, the signal intensity of NO reaches that of the feed, indicating the cease of all adsorption and/or reaction processes.

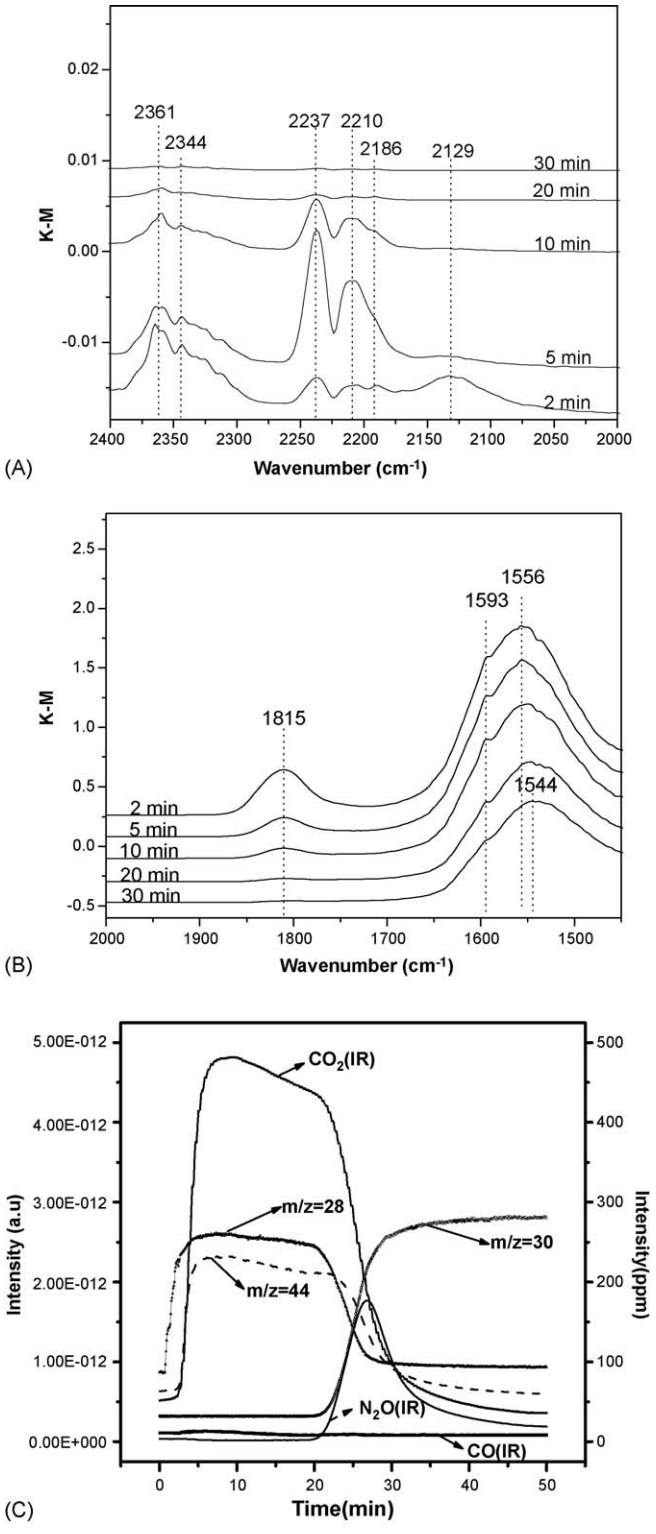

Fig. 2. DRIFT spectra ((A) 2400–2000 cm^{-1} and (B) 2000–1300 cm^{-1}) as a function of time when a NiO/CeO_2 sample pre-treated with 1% CO/He was exposed to 1% NO/He at 170 °C. IR responses of gas phase CO, CO_2, N_2O, and MS signals at m/z = 28, 30, 32 and 44 obtained when a NiO/CeO_2 catalyst pre-treated with 0.08% CO/Ar was exposed to 0.08% NO/Ar at 170 °C (C).

3.1.3. NO adsorption on NiO/CeO_2 catalyst

The DRIFTS spectra obtained following exposure of NiO/CeO_2 catalyst to 1% NO/He at 170 °C are shown in Fig. 3(A). There are

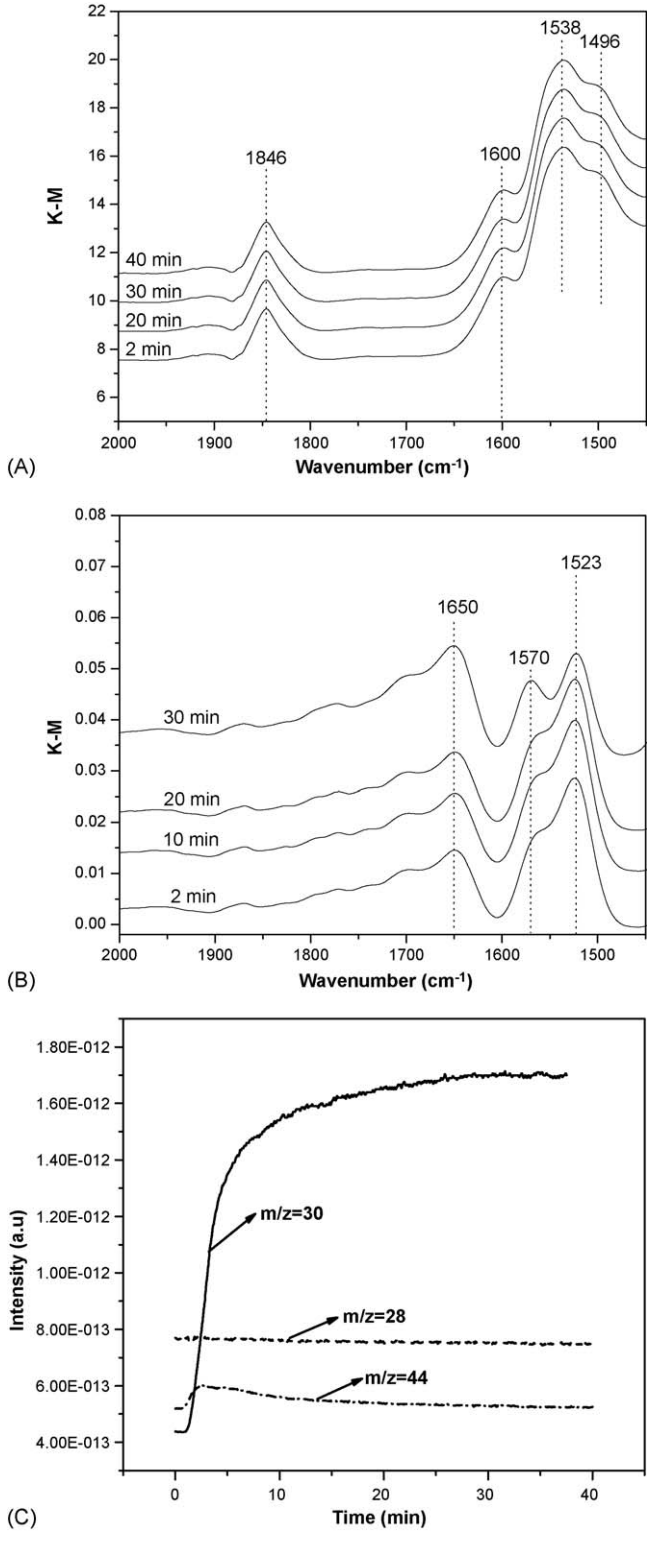

Fig. 3. DRIFT spectra (2400–2000 cm^{-1}) as a function of time when NiO/CeO_2 (A) and CeO_2 (B) was exposed to 1% NO/He; and mass signals at m/z = 28, 30 and 44 obtained when NiO/CeO_2 was exposed to a flow of 0.08% NO/Ar at 170 °C (C).

strong and overlapped bands at 1600, 1538, and 1496 cm^{-1} in the 1650–1450 cm^{-1} region, and a band at 1846 cm^{-1} is also observed. In the case of CeO_2 exposure to 1% NO/He (Fig. 3(B)), the band at 1846 cm^{-1} does not appear whereas the strong bands at 1650, 1570, and 1523 cm^{-1} are observed.

In agreement with the work conducted by other researchers [36], the band at 1846 cm^{-1} (not observed over pure CeO_2) can be safely assigned to NO adsorbed on Ni^{2+}. The bands located in the 1650–1450 cm^{-1} region should be ascribed to adsorbed NO_x (x = 2 or 3) [[22] and the references therein]. The differences in wave numbers of NO_x over NiO/CeO_2 and CeO_2 should be due to discrepancies of NO_x interaction with adsorbents. Similar experiments have been conducted by employing an online MS. As shown in Fig. 3(C), after 1 min, there is the detection of NO and N_2O, the signal of the latter comes to a maximum at 2.3 min and declines as the signal of NO increases to its full capacity in a period of ca. 30 min.

3.1.4. CO interaction with NO pre-treated catalyst

Experimental results obtained following the "first NO then CO" mode over NiO/CeO_2 catalyst at 170 °C are presented in Fig. 4(A and B). Exposing the sample pre-treated with NO to 1% CO/He results in the progressive disappearance of the band at 1820 cm^{-1}, while the bands at 2363 and 2335 cm^{-1} as well as the bands at 2186, 2173 and 2117 cm^{-1} gradually increase with time on steam. Apart from the bands mentioned above, the bands below 1650 cm^{-1} also increase in intensity.

The peak at 1846 cm^{-1} which has been assigned to NO adsorbed on Ni^{2+} shifts to 1820 cm^{-1} after exposure to CO. The red shift should be due to partial reduction of Ni^{2+} to Ni^{+} by CO. The peak disappears after 40 min of CO exposure. The bands at 2363 and 2335 cm^{-1} (ascribable to adsorbed CO_2) and the bands at 2186, 2173 and 2117 cm^{-1} (attributable to CO on adsorbents) are similar to those of Fig. 1(A). The bands below 1650 cm^{-1} are ascribed to carbonates complexes. It is noted that Hungria et al. [5] ascribed the band at 1575 cm^{-1} to bidentate carbonates while that at 1496 cm^{-1} ascribed to monodentate carbonates.

The results of the corresponding MS-IRAS experiments are presented in Fig. 4(C). It is observed that there are CO_2 and NO detection after an on-stream time of ca. 2 min. At 10 min, the signals of CO_2 and NO decrease while that of CO appears. After about 35 min, the signal of CO reaches its full capacity, indicating the end of CO adsorption.

3.1.5. Co-adsorption of NO and CO

The DRIFTS spectra of the co-adsorption of NO and CO on NiO/CeO_2 catalyst at 170 °C are shown in Fig. 5(A and B). It is observed that after exposure to the NO–CO mixture, the intense bands which are attributed to the N_2O (2237 cm^{-1}) and NCO species (2210 cm^{-1}) appear immediately. The bands come to a maximum after 10 min and remain unchanged with time on steam. The development of these bands coincides with the appearance and development of the band at 1815 cm^{-1} that has been ascribed to the vibration of Ni^{+}–NO species. The band at 2129 cm^{-1} due to the vibration of surface CO species [36] appears after ca. 10 min and gradually develops with time. The stability of the species formed on the catalyst surface was investigated by means of having the sample purged with a flow of He for 2 min. It is observed that the bands of N_2O (2237 cm^{-1}) and NCO species (2210 cm^{-1}) disappear immediately upon He purging while the CO band at 2129 cm^{-1} remains uncharged. It is also observed that the Ni^{+}–NO band at 1815 cm^{-1} decreases in intensity but is not completely removed after 2 min of He purging.

The corresponding MS-IRAS experiments were conducted. As observed in Fig. 5(C), at the initial stage of exposure to 0.5% CO–0.5% NO/He only N_2 is detected at the exit. After ca. 7 min, the production of N_2O (accompanied by the desorption of NO) increases with time and comes to a maximum after ca. 11 min. While the generation of N_2 shows a slight decrease during this process. After ca. 14 min, the release of CO_2 (coinciding with the increase of N_2) appears and progressively increases with

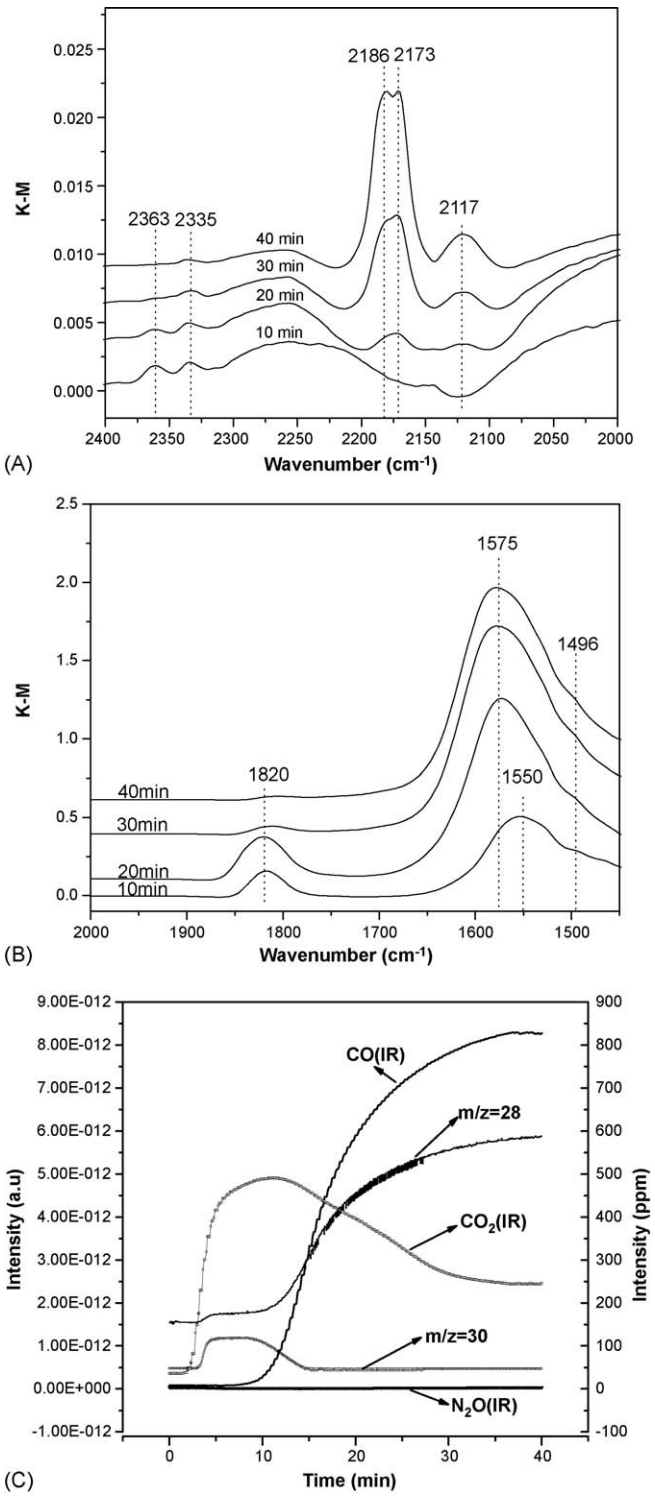

Fig. 4. DRIFT spectra ((A) 2400–2000 cm^{-1} and (B) 2000–1300 cm^{-1}) as a function of time when NiO/CeO_2 pre-treated with 1% NO/He was exposed to 1% CO/He at 170 °C. IR responses of gas phase CO, CO_2, N_2O, and MS signals at m/z = 28, 30 and 44 obtained when NiO/CeO_2 pre-treated with 0.08% NO/Ar was exposed to 0.08% CO/Ar at 170 °C (C).

time. At about 20 min, the signal of N_2 and CO_2 reach their full capability, indicating the NO–CO reaction has reached a steady state. The TPD spectrum that followed is presented in Fig. 5(D). The desorption profile of CO_2 exhibits two maxima at 210 and 260 °C, and there is no desorption of N_2O, NO and CO.

3.2. Thermal stability and reactivity of NCO species

3.2.1. Thermal stability

The DRIFT spectra obtained after interaction of NiO/CeO_2 catalyst with 0.5% CO–0.5% NO/He as a function of temperature are shown in Fig. 6. The catalyst was first exposed to the gas mixture at 100 °C, then the temperature was stepwise increased, and the spectra were obtained after steady state was reached. It is observed that interaction of NO and CO with the catalyst leads to the formation of several surface species, and the population of which depends on temperature. Below 170 °C, the spectra were dominated by signals of N_2O (2237 cm^{-1}) and NCO complexes (2210 cm^{-1}). The intensities of these bands go through a maximum in the 150–170 °C range and decrease to near zero at 210 °C. Nonetheless, the band at 2129 cm^{-1} due to adsorbed CO appears to be highly stable in this temperature range.

3.2.2. Reactivity towards NO

The DRIFT spectra obtained upon interaction of NCO species (formed under 0.5% CO–0.5% NO/He reaction conditions) with 0.08% NO/He are presented in Fig. 7(A and B). Switching the feed to 0.08% NO/He results in the immediate disappearance of the band at 2237 cm^{-1} (N_2O) and the band at 2210 cm^{-1} (NCO species). The intense band at 2129 cm^{-1} attributable to Ni^+–CO, gradually decreases and disappears after about 10 min. As for the Ni^+–NO band at 1815 cm^{-1}, it also gradually decreases and disappears within 20 min.

The corresponding MS-IRAS results are shown in Fig. 7(C). Upon introduction of 0.08% NO/He, there is the production of N_2 and CO_2 at ca. 2 min. After ca. 6 min, the yield of N_2 reaches maximum and then starts to fall. At the same time, the formation of N_2O (accompanied by NO desorption) starts and peaks at ca. 11 min. After 30 min, the signal intensity of NO reaches that of the feed, indicating the cease of all adsorption and reaction activities.

In the subsequent TPD experiments (Fig. 7(D)), one can see that the evolution of N_2 peaks at 260 °C, coinciding with that of CO_2. The NO profile displays two maxima, one at ca. 260 °C and the other at 420 °C. The former can be ascribed to strongly adsorbed NO while the latter (accompanied with the release of O_2) to the NO generated due to NO_x (x = 2, 3) decomposition.

3.2.3. Reactivity towards CO

The DRIFT spectra obtained upon interaction of NCO species (formed under 0.5% CO–0.5% NO/He reaction conditions) with 0.08% CO/He are presented in Fig. 8(A and B). Switching to 0.08% CO/He results in the immediate disappearance of the 2237 cm^{-1} band (N_2O) and the 2210 cm^{-1} band (NCO species). In the mean time, there is the development of the Ni^+–CO band at 2129 cm^{-1} and the decrease of the Ni^+–NO band at 1815 cm^{-1}.

The corresponding MS-IRAS results are shown in Fig. 8(C). Introduction of 0.08% CO/He leads to the production of relatively small amount of N_2 and CO_2, and there is no generation of N_2O and NO. The signal of CO gradually increases and reaches that of the feed.

In the subsequent TPD experiments (Fig. 8(D)), one can see that the CO_2 profile displays two maxima, one at ca. 260 °C and the other 375 °C. The m/z = 28 signal of lower intensity exhibits a profile similar as that of m/z = 44 and CO_2 (IR), indicating that m/z = 28 signal is due to CO_2 cracking. There is a minute amount of CO but no detection of NO and N_2.

4. Discussion

4.1. Interaction of NO with CO pre-treated catalyst

As shown in Fig. 1(A), with the exposure of the NiO/CeO_2 to 1% CO/He at 170 °C, there is the formation of surface CO_2, and the

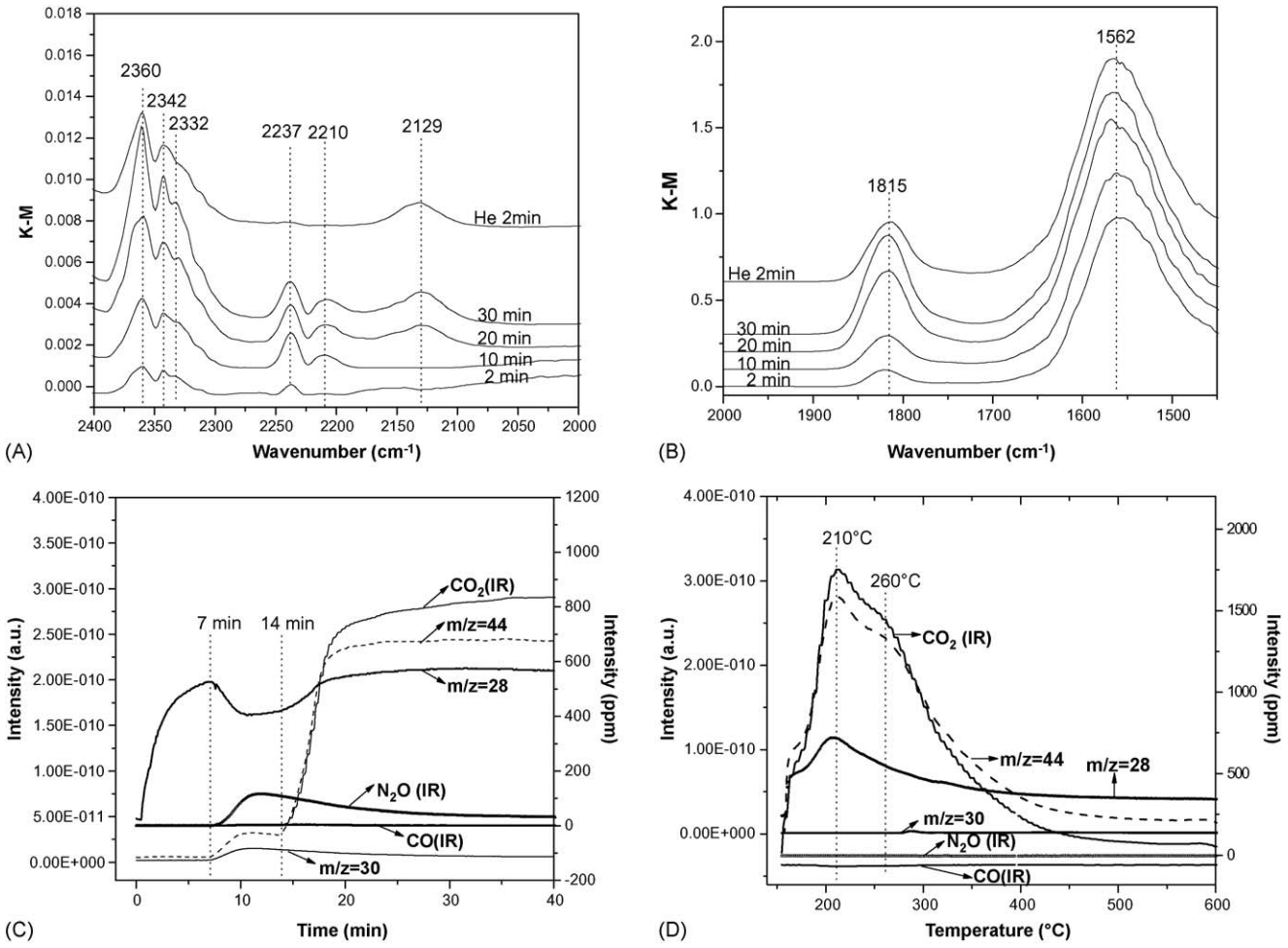

Fig. 5. DRIFT spectra ((A) 2400–2000 cm^{-1} and (B) 2000–1300 cm^{-1}) as a function of time when NiO/CeO_2 was exposed to 0.5% CO–0.5% NO/He at 170 °C. IR responses of gas phase CO, CO_2, N_2O, and MS signals at m/z = 28, 30 and 44 obtained when NiO/CeO_2 was exposed to 0.5% CO–0.5% NO/He at 170 °C (C), followed by purging with He and subsequent TPD of adsorbed species (D).

concentration of CO_2 decreases with time of exposure. The bands due to vibration of adsorbed CO species do not appear immediately upon exposure of the catalyst to CO, but develop when the bands due to adsorbed CO_2 begin to decrease in intensity. Upon saturated adsorption, CO is the dominant surface species.

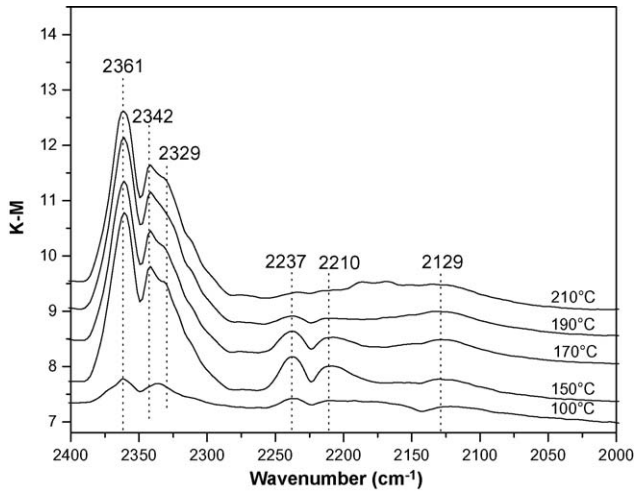

Fig. 6. DRIFT spectra (2400–2000 cm^{-1}) as a function of temperature when NiO/CeO_2 was exposed to 0.5% CO–0.5% NO/He.

Comparing Fig. 1(A) with (B), it is obvious that there is no CO_2 generation over pure CeO_2, indicating that the reduction of surface oxygen by CO does not occur at 170 °C over pure CeO_2. However, there is obvious reduction of surface oxygen by CO over NiO/CeO_2 catalyst. The results imply that the loading of NiO on ceria leads to the generation of oxygen species that can be easily reduced. The presence of this kind of oxygen species is considered as the reason for the high catalytic activities of the NiO/CeO_2 catalyst.

In accordance with the MS results (Fig. 1(C)), CO_2 is generated when CO interacts with NiO/CeO_2 catalyst. With time on stream, the catalyst surface is depleted of oxygen species that are easily reducible and the yield of CO_2 decreases. In the meantime the level of gaseous CO at the exit of the reactor progressively reaches that of the feed.

The process can be described as follows (*denotes a vacant site):

$$CO + * \rightarrow *CO \quad (1)$$

$$*CO + *O \rightarrow CO_2 + 2* \quad (2)$$

Exposing the catalyst pre-treated with CO to NO results in distinct changes in DRIFTS profile (Fig. 2(A and B)). The bands due to surface CO species disappear, and a new band at 2210 cm^{-1} due to the NCO species is clearly observed. The formation of NCO species has been proposed to occur in the reaction of adsorbed CO with surface nitrogen atoms produced in NO dissociative chemisorption. In other words, the detection of surface NCO intermediates provides obvious evidence that NO dissociates into

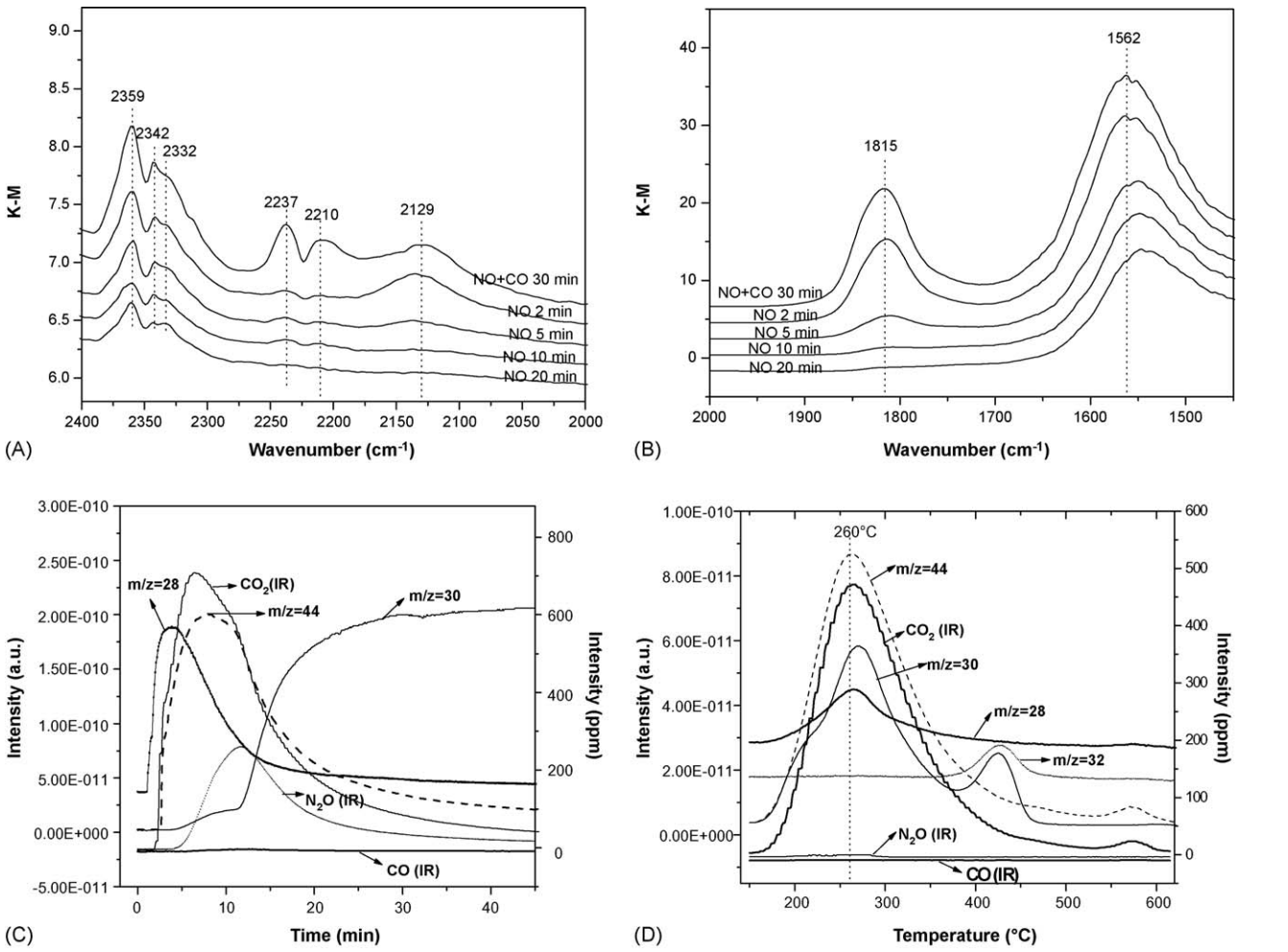

Fig. 7. DRIFT spectra ((A) 2400–2000 cm^{-1} and (B) 2000–1300 cm^{-1}) as a function of time when NiO/CeO_2 pre-treated with 0.5% CO–0.5% NO/He was exposed to 0.08% NO/He at 170 °C. IR responses of gas phase CO, CO_2, N_2O, and MS signals at m/z = 28, 30 and 44 obtained when NiO/CeO_2 pre-treated with 0.5% CO–0.5% NO/He was exposed to 0.08% NO/He at 170 °C (C), followed by purging with He and subsequent TPD of adsorbed species (D).

*N and *O over the NiO/CeO_2 catalyst pre-reduced by CO.

$$NO + * \rightarrow *NO \quad (3)$$

$$*NO + * \rightarrow *N + *O \quad (4)$$

$$*N + *CO \rightarrow *NCO + * \quad (5)$$

The DRIFTS results reported so far correlate well with the corresponding MS results. As shown in Fig. 2(C), upon exposure of the catalyst pre-treated with CO to NO, there is immediate detection of N_2 followed by the generation of significant amount of CO_2. The formation of N_2 and CO_2 is via the reactions:

$$*N + *N \rightarrow N_2 + 2* \quad (6)$$

$$*O + *CO \rightarrow CO_2 + 2* \quad (7)$$

With the combination of surface N atoms, there is the formation of surface N_2 that desorbs readily to the gas phase. In the mean time, there is the detection of N_2O and NO at the exit of the reactor. It should be noted that the dissociative adsorption of NO also results in the accumulation of surface oxygen atoms as reflected in the progressive decrease of N_2 yield. Simultaneously, there is the formation of N_2O and the appearance of gaseous NO in the effluent of the reactor. With the depletion of surface *N, the reaction between *NO and *N (yielding N_2O) ceases, and the signal intensity of NO reaches that of the feed.

$$*N + *NO \rightarrow N_2O + 2* \quad (8)$$

Since we detect no desorption of CO, we deduce that there is no direct replacement of surface CO by the incoming NO molecules. In other words, most of the surface CO ends up as *NCO or CO_2.

4.2. Interaction of CO with NO pre-treated catalyst

According to the results of Fig. 3(A), with the exposure of the NiO/CeO_2 catalyst to 1% NO/He at 170 °C, there are two modes of NO adsorption: one is in the form of *NO and the other in the form of $*NO_x$ (x = 2 or 3).

$$(9) NO + * \leftrightarrow *NO$$

$$(10) NO + x*O \leftrightarrow *NO_x$$

As shown in Fig. 3(C), the interaction of NO with NiO/CeO_2 results in the formation of N_2O. According to Martinez-Arias et al. [42], when two NO molecules are located closely at a Ce^{3+}-oxygen vacant site, there is the formation of hyponitrite, and the decomposition of hyponitrite would result in the evolution of N_2O. Reactions (11) and (12) account for the formation of N_2O:

$$2NO + * \leftrightarrow NO*NO \quad (11)$$

$$NO*NO \leftrightarrow N_2O + *O \quad (12)$$

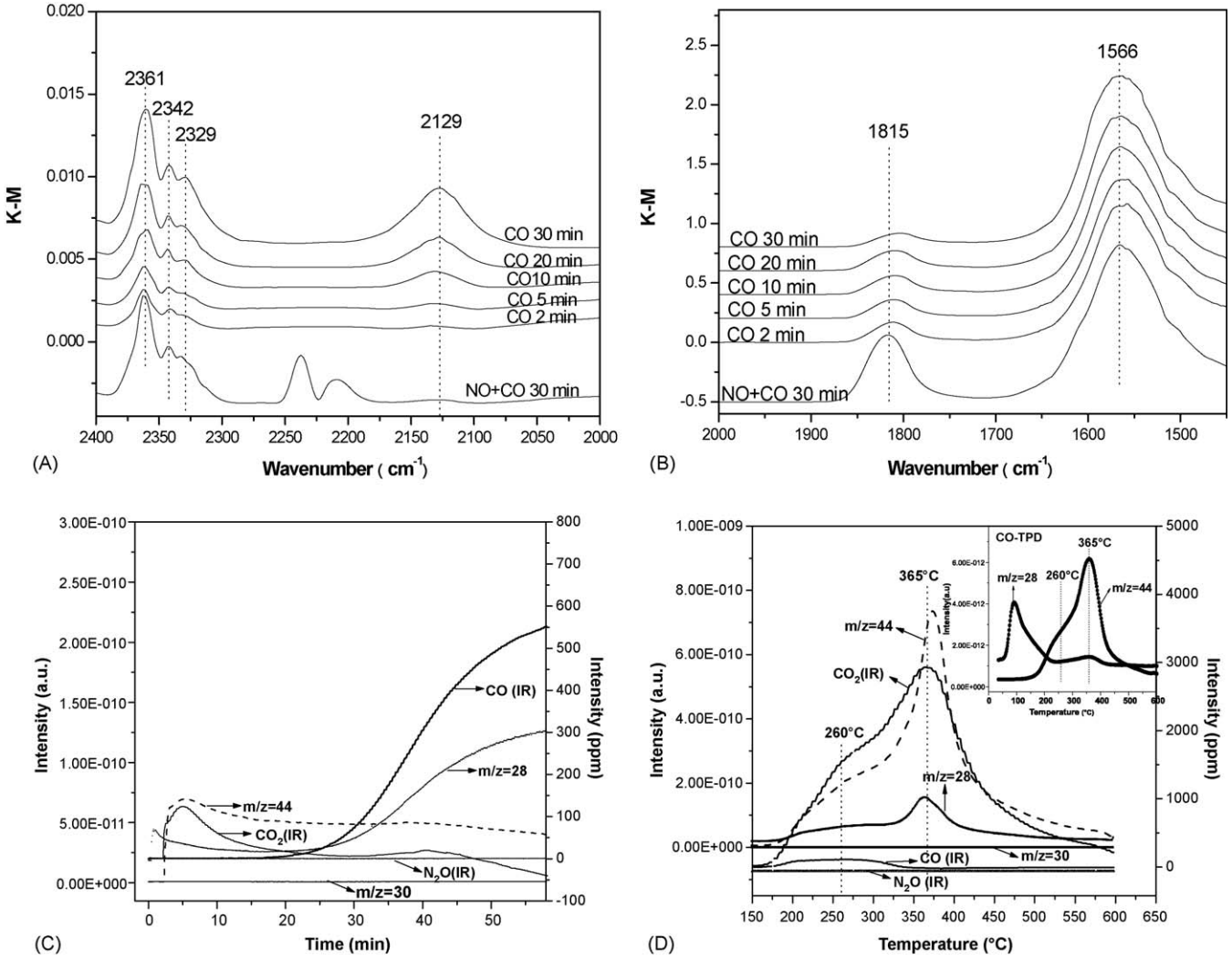

Fig. 8. DRIFT spectra ((A) 2400–2000 cm^{-1} and (B) 2000–1300 cm^{-1}) as a function of time when NiO/CeO_2 pre-treated with 0.5% CO–0.5% NO/He was exposed to 0.08% CO/He at 170 °C. IR responses of gas phase CO, CO_2, N_2O, and MS signals at m/z = 28, 30 and 44 obtained when NiO/CeO_2 pre-treated with 0.5% CO-0.5% NO/He was exposed to 0.08% CO/He at 170 °C (C), followed by purging with He and subsequent TPD of adsorbed species (D).

With the occupancy of active sites by surface oxygen atoms, there is the gradual decline in N_2O generation. Since there is no N_2 production during the NO adsorption process, one can deduce that NO adsorption on calcined NiO/CeO_2 is associative.

As shown in Fig. 4(A and B), the results of CO interaction with a catalyst pre-covered with NO at 170 °C leads to gradual displacement of the band at 1820 cm^{-1} and the appearance of ν(C–O) bands. The appearance of the bands at 2363 and 2335 cm^{-1} (due to adsorbed CO_2) evidences that the catalyst has been partially oxidized. With increase of CO exposure, there is the appearance of the bands at 2186, 2173 and 2117 cm^{-1} ascribable to surface CO. In contrast to the case of "first CO then NO", there is no formation of NCO when a NiO/CeO_2 surface pre-treated with NO is exposed to CO. The fast generation of gaseous CO_2 (Fig. 4(C)) suggests that there is partial oxidation of catalyst during NO pre-treatment. The detection of gaseous NO implies that the surface NO and NO_x species can be replaced by the incoming CO. Besides CO_2 and NO, there is no production of other gaseous species such as N_2.

$$*CO + *O \rightarrow CO_2 + 2* \quad (13)$$

$$CO + *NO \rightarrow NO + *CO \quad (14)$$

$$*CO + *NO_x \rightarrow NO + CO + x*O \quad (15)$$

With time on stream, the catalyst surface is depleted of *O, *NO and $*NO_x$, and the generation of CO_2 gradually drops. The CO_2 profile shows a long tail, suggesting that the incoming CO also interacts with the oxygen atoms of ceria:

$$CeO_2 + xCO \rightarrow CeO_{2-x} + xCO_2 \quad (16)$$

Based on the points discussed so far, it is clear that during the NO adsorption process, NO does not dissociate to produce nitrogen atoms over an oxidized NiO/CeO_2 surface. When CO interacts with the adsorbed NO, there is no formation of N_2, suggesting that neither *NO nor $*NO_x$ species react directly with CO to produce N_2. In other words, it is not feasible to have NO reduced by CO via such a route. On the other hand, during NO interaction with the catalyst pre-treated with CO, there is the production of NCO complexes and N_2, indicating that removal of surface oxygen for generation of vacancies via CO reduction is the first and crucial step, and the dissociation of NO on the reduced surface is the pathway for N_2 generation.

4.3. Co-adsorption of NO and CO on NiO/CeO_2

The DRIFTS results of the co-adsorption of NO and CO on NiO/CeO_2 at 170 °C (Fig. 5(A and B)) confirm that there is the generation

of surface NCO, Ni^+–CO and Ni^+–NO as well as gaseous CO_2 and N_2O. Similar products are observed when NiO/CeO_2 pre-treated with CO is exposed to NO (Section 4.1). Based on the results of NO interaction with CO pre-treated catalyst, one can figure out the reaction mechanism of co-adsorption.

According to the MS results (Fig. 5(C)), the NO–CO reaction process can be divided into three stages. In the first stage (within ca. 7 min), CO reduces surface oxygen to produce CO_2, resulting in active sites suitable for NO dissociative adsorption. In this period, there is rapid release of N_2 (g) and formation of surface CO_2 on the catalyst. In the second stage (from 7 to 14 min), with the occupancy of active sites by *O, the dissociation of adsorbed NO is hindered. As a result, the yield of N_2 declines and the formation of N_2O begins. In the third stage (after ca. 14 min), the reaction reaches its steady stage. It is likely that a redox cycle is established in this catalytic system.

4.4. Thermal stability of NCO species

The DRIFTS results of Fig. 5(A) show that the NCO species formed in co-adsorption of NO and CO at 170 °C has low stability and disappears immediately upon purging with He at this temperature. In terms of thermal stability, the band of NCO species (2210 cm^{-1}) disappears at 210 °C (Fig. 6), and the profile of CO_2 desorption has two components, one at 210 °C (accompanied with N_2 desorption) and the other at ca. 260 °C (Fig. 5(D)). According to Kondarides et al. [22], Rh-NCO species decompose to produce Rh-CO and Rh-N species, yielding N_2 and CO_2 at the same time. In accordance with these results, we attribute the CO_2 at 210 °C to the decomposition of NCO species. The process can be described as follows:

$$*NCO + * \rightarrow *CO + *N \quad (17)$$

$$*CO + *O \rightarrow CO_2 + 2* \quad (18)$$

$$*N + *N \rightarrow N_2 + 2* \quad (19)$$

The CO_2 desorbed at 260 °C can be ascribed to the CO_2 generated via the interaction of CO with surface oxygen:

$$*O + *CO \rightarrow CO_2 + 2* \quad (20)$$

4.5. Reactivity of NCO species

4.5.1. Reactivity with NO

The reactivity of NCO species with NO has been studied by a number of investigators, and in some cases N_2O and CO are suggested to be the final products [23,43]. While, others suggested that NCO interaction with NO could lead to the formation of N_2 and CO_2 [39,44–46]. In our investigation, the band (2210 cm^{-1}) due to NCO species disappears upon exposure to 0.08% NO/He (Fig. 7(A and B)). In the gas phase (Fig. 7(C)), immediately after exposure to NO, N_2 and CO_2 are detected in large amount but there is no detection of N_2O and CO at the exit of the reactor. When the yield of N_2 starts to decline, N_2O formation begins and peaks at ca. 11 min on stream, coinciding with the profile of CO_2 generation. Similar phenomenon is observed when NiO/CeO_2 pre-treated with CO is exposed to NO. We hence suggest that the NCO species can react with NO to produce N_2 and CO_2.

$$*NCO + NO \rightarrow CO_2 + N_2 + * \quad (21)$$

In the subsequent TPD experiments (Fig. 7(D)), one can see that the evolution of N_2 coincides with that of CO_2, both come to a maximum at 260 °C. Similar phenomena are observed when NiO/CeO_2 pre-exposed to a mixture of NO and CO is subject to TPD treatment (Fig. 5(D)). Since there is no CO_2 desorption at 210 °C, we conclude that the generation of CO_2 and N_2 that maximizes at 260 °C is not due to the decomposition of surface NCO but rather due to the interaction of CO and NO on the surface. In other words, the interaction of NCO with NO happens at temperatures lower than 260 °C, likely to be in the 170–210 °C range.

4.5.2. Reactivity with CO

As shown in Fig. 8(A and B), the introduction of 0.08% CO/He flow (at 170 °C) to the NiO/CeO_2 catalyst previously exposed to 0.5% CO–0.5% NO/He causes the disappearance of the NCO band. Since similar phenomenon has been observed when the sample is subject to He purging, it is suggested that the removal of NCO is due to purging rather than a result of chemical interaction. The fact that the Ni^+–CO (2129 cm^{-1}) band gradually increases with time of CO exposure and shows high stability, while the Ni^+–NO band (1815 cm^{-1}) gradually decreases suggests that there is replacement of NO by CO, and the interaction of CO with surface NCO is insignificant. In the gas phase (Fig. 8(C)), we detect small amount of N_2 and CO_2, much lower than that observed in the interaction of NCO with NO (Fig. 7(C)). Thus, the formation of these products is due to the reduction of surface oxygen by the introduced CO, producing "oxygen vacant" sites for the dissociation of NO and the final yielding of N_2 and CO_2. In agreement with the reports of Kondarides et al. [22,23], the NCO species do not interact directly with CO.

In the subsequent TPD experiments (Fig. 8(D)), one can see that the CO_2 profiles display a peak at ca. 365 °C with a shoulder at 260 °C. In a CO-TPD experiment separately performed over the catalyst, a similar CO_2 desorption profile is obtained (inset of Fig. 8(D)). Thus, it is reasonable to deduce that the generation of CO_2 is a result of CO interaction with various kinds of surface oxygen species. Similar deduction has been made by Chary et al. [47]. The $m/z = 28$ signal of lower intensity that peaks at about 365 °C shows a profile similar to that of $m/z = 44$. Since we do not detect the release of N_2 above 350 °C in the other TPD investigations reported herein, we ascribe the $m/z = 28$ signal to part of the cracking pattern of CO_2. The related reactions can be illustrated as:

$$*O + *CO \rightarrow CO_2 + 2* \quad (22)$$

$$CeO_2 + xCO \rightarrow CeO_{2-x} + xCO_2 \quad (23)$$

5. Conclusions

Based on the results delivered so far, one can see that NCO species are formed when CO adsorbed on NiO/CeO_2 is exposed to NO. It is a result of CO interaction with the nitrogen atoms generated in NO dissociation. The generation of NCO can be realized by means of exposing pre-adsorbed CO to NO or by means of co-adsorption of CO and NO on NiO/CeO_2. The exposure of the catalyst first to NO and then to CO does not result in the formation of NCO. The interaction of NO with NCO on NiO/CeO_2 produces gaseous N_2 and CO_2. The interaction of NO with NiO_2/CeO_2, however, produces surface NO and NO_x, and the interaction of CO with these species produces gaseous NO and CO_2 rather than N_2. Being low in thermal stability, NCO decomposes to produce *CO and *N species, and finally yielding N_2 and CO_2. In other words, isocyanates do not interact directly with CO but rather react with NO to yield N_2 and CO_2. The reaction steps of NO reduction by CO over NiO_2/CeO_2 are suggested to be: (i) removal of surface oxygen by CO to create vacant sites; (ii) NO dissociation to produce N_2 on the vacant sites; (iii) oxygen originated from NO dissociation is reduced by CO to regenerate surface vacant sites.

Acknowledgements

The work was supported by the National Natural Science Foundation of China (Nos. 20573014 and 20077005) and by the Program for New Century Excellent Talents in University (NCET-07-0136), as well as by the National High Technology and Development Program (863 program) of China (Grant No. 2007AA06Z311).

References

[1] M. Shelef, G.W. Graham, Catal. Rev. Sci. Eng. 36 (1994) 433–457.
[2] J.N. Armor, Appl. Catal. B 1 (1992) 221–256.
[3] K.C. Taylor, Catal. Rev. Sci. Eng. 35 (1993) 457–481.
[4] A.B. Hungria, J.J. Calrino, J.A. Anderson, A. Martinez-Arias, Appl. Catal. B 62 (2006) 359–368.
[5] A.B. Hungria, N.D. Browning, R.P. Erni, M. Fernandez-Garcia, J.C. Conesa, J.A. Perez-Omil, A. Martinez-Arias, J. Catal. 235 (2005) 251–261.
[6] T. Ohno, F. Hatayama, Y. Toda, S. Konishi, H. Miyata, Appl. Catal. B 5 (1994) 89–101.
[7] T. Ohno, Y. Bunno, F. Hatayama, Y. Toda, H. Miyata, Appl. Catal. B 30 (2001) 421–428.
[8] Y.H. Hu, L. Dong, M.M. Shen, D. Liu, J. Wang, W.P. Ding, Y. Chen, Appl. Catal. B 31 (2001) 61–69.
[9] L. Ma, M.F. Luo, S.Y. Chen, Appl. Catal. A 242 (2003) 151–159.
[10] X.Y. Jiang, L.P. Lou, Y.X. Chen, X.M. Zheng, J. Mol. Catal. A 197 (2003) 193–205.
[11] A. Martínez-Arias, M. Fernández-García, J. Soria, J.C. Conesa, J. Catal. 214 (2003) 261–272.
[12] E.F. Iliopoulou, E.A. Efthimiadis, I.A. Vasalos, Ind. Eng. Chem. Res. 43 (2004) 1388–1394.
[13] E.F. Iliopoulou, A.P. Evdou, A.A. Lemonidou, I.A. Vasalos, Appl. Catal. A 274 (2004) 179–189.
[14] N.A.S. Amin, E.F. Tan, Z.A. Manan, Appl. Catal. B 43 (2003) 57–69.
[15] M. Fernández-García, A. Martínez-Arias, A. Iglesias-Juez, A.B. Hungría, J.A. Anderson, J.C. Conesa, J. Soria, J. Catal. 214 (2003) 220–233.
[16] C.Y. Lee, T.H. Jung, B.H. Ha, Appl. Catal. B 9 (1996) 77–91.
[17] L.F. Liotta, G. Pantaleo, G. Di Carlo, G. Marci, G. Deganello, Appl. Catal. B 52 (2004) 1–10.
[18] Y. Wang, A.M. Zhu, Y.Z. Zhang, C.T. Au, X.F. Yang, C. Shi, Appl. Catal. B 81 (2008) 141–149.
[19] K. Almusaiteer, S.S.C. Chuang, J. Catal. 184 (1999) 189–201.
[20] K. Almusaiteer, R. Krishnamurthy, S.S.C. Chuang, Catal. Today 55 (2000) 291–299.
[21] T. Chafik, D.I. Kondarides, X.E. Verykios, J. Catal. 190 (2000) 446–459.
[22] D.I. Kondarides, T. Chafik, X.E. Verykios, J. Catal. 191 (2000) 147–164.
[23] D.I. Kondarides, T. Chafik, X.E. Verykios, J. Catal. 193 (2000) 303–307.
[24] T. Bánsági, T.S. Zakar, F. Solymosi, Appl. Catal. B 66 (2006) 147–150.
[25] P. Granger, L. Delannoy, J.J. Lecomte, C. Dathy, H. Praliaud, L. Leclercq, G. Leclercq, J. Catal. 207 (2002) 202–212.
[26] D. Chatterjee, O. Deutschmann, J. Warnatz, Faraday Discuss 119 (2002) 371–384.
[27] S. Roy, A. Marimuthu, M.S. Hegde, G. Madras, Appl. Catal. B 71 (2007) 23–31.
[28] T. Baidya, A. Marimuthu, M.S. Hegde, N. Ravishankar, G. Madras, J. Phys. Chem. C 111 (2007) 830–839.
[29] S.S.C. Chuang, C.-D. Tan, J. Catal. 173 (1998) 95–104.
[30] A.R. Balkenende, C.J.G. Van der Gift, E.A. Meulenkamp, J.W. Geus, Appl. Surf. Sci. 68 (1993) 161–171.
[31] A.T.S. Wee, J. Lin, A.C.H. Huan, F.C. Loh, K.L. Tan, Surf. Sci. 304 (1994) 145–158.
[32] F. Boccuzzi, M. Baricco, E. Guglielminotti, Appl. Surf. Sci. 70–71 (1993) 147–152.
[33] F. Boccuzzi, E. Guglielminotti, G. Martra, G. Gerrato, J. Catal. 146 (1994) 449–459.
[34] V.I. Pârvulescu, P. Grange, B. Delmon, Catal. Today 46 (1998) 233–316.
[35] C. Kladis, S.K. Bhargava, K. Foger, D.B. Akolekar, J. Mol. Catal. A 175 (2001) 241–248.
[36] M. Mihaylov, K. Chakarova, K. Hadjiivanov, J. Catal. 228 (2004) 273–281.
[37] T. Szailer, J.H. Kwak, D.H. Kim, J.C. Hanson, C.H.F. Peden, J. Szanyi, J. Catal. 239 (2006) 51–64.
[38] M. Haneda, Y. Kintaichi, M. Inaba, H. Hamada, Catal. Today 42 (1998) 127–135.
[39] F. Solymosi, T. Bánsági, T.S. Zakar, Catal. Lett. 87 (2003) 7–10.
[40] F. Solymosi, T. Bánsági, T.S. Zakar, Phys. Chem. Chem. Phys. 5 (2003) 4724–4730.
[41] T. Venkov, K. Hadjiivanov, D. Klissurski, Phys. Chem. Chem. Phys. 4 (2002) 2443–2448.
[42] A. Martinez-Arias, J. Soria, J.C. Conesa, X.L. Seoane, A. Arcoya, R. Cataluna, J. Chem. Soc., Faraday Trans. 91 (1995) 1679–1687.
[43] J. Goslara, M. Wojciechowskab, M. Zielińskib, J. Phys. Chem. Solids 67 (2006) 1387–1393.
[44] E.F. Iliopoulou, E.A. Efthimiadis, L. Nalbandian, I.A. Vasalos, J.-O. Barth, J.A. Lercher, Appl. Catal. B 60 (2005) 277–288.
[45] O.S. Alexeev, S. Krishnamoorthy, C. Jensen, M.S. Ziebarth, G. Yaluris, T.G. Roberie, M.D. Amiridis, Catal. Today 127 (2007) 189–198.
[46] T. Fujitani, I. Nakamura, A. Takahashi, M. Haneda, H. Hamada, J. Catal. 253 (2008) 139–147.
[47] K.V.R. Chary, P.V.R. Rao, V. Vishwanathan, Catal. Commun. 7 (2006) 974–978.